Late Paleozoic Iberian orocline(s) require 1000 km of missing intra-Pangea shortening.

Daniel Pastor-Galán[1,3]

Emilio L. Pueyo[2]

Mark Diederen[3]

Cristina García-Lasanta[4]

Cor G. Langereis[3]

[1] CNEAS, Tohoku University, 41 Kawauchi, Aoba-ku, Sendai, Japan

[2] Instituto Geológico y Minero de España, Unidad de Zaragoza, C/Manuel Lasala 44, 9°, 50006 Zaragoza, Spain

[3] Faculty of Geosciences, Utrecht University, P.O. Box 80021, 3508 TA, Utrecht, The Netherlands

[4] Universidad de Zaragoza, Pedro Cerbuna 12, 50009 Zaragoza Spain

Abstract

Supercontinents are usually interpreted to be single and rigid continental plates. How and when Pangea became a rigid supercontinent is disputed and age estimations vary from 330 to 240 Ma. The Gondwana-Laurussia collision formed the Variscan-Alleghanian belt, the most prominent witness of Pangea's amalgamation. In Iberia, this orogen draws an "S" shape featured by the Cantabrian Orocline and the Central Iberian curve. The curvature of Central Iberian is particularly evident in the Morais Complex and in a change of trend that it draws in the Aragonese Branch of the Iberian Range. Recent research showed that both curvatures are not coeval and that the Central Iberian had to form prior to 318 Ma. We report paleomagnetic and structural results from Paleozoic rocks in the Santa Cruz syncline (Aragonese Branch of the Iberian Range) that indicate two main vertical axis rotations events: 1) a Cenozoic (Alpine) clockwise rotation of >20˚ and 2) a Late Carboniferous counterclockwise rotation of ~70˚. Once restored the Cenozoic rotation, the change

in structural trend that allegedly evidence the outer arc of the Central Iberian curve disappears. Whereas the Cenozoic rotation is incompatible with a Central Iberian curve, the Late Carboniferous rotation is fully compatible with the Cantabrian Orocline, enlarging the area affected by its counterclockwise rotations. Using our results we reconstruct the Iberian rotation during the Paleozoic with Gplates and quantified the amount of convergence accommodated in the core of Pangea due to this process to be a minimum of 1000 km.

Keywords: Pangea, Iberian Range, Central Iberian curve, Variscan, Paleomagnetism.

1 Introduction

Supercontinents are interpreted to be single continental plates of a size capable of influencing mantle convection patterns and even core-mantle boundary processes (Pastor-Galán et al., in press a). The amalgamation and break-up of Pangea, the latest supercontinent, are the geologists' template for the supercontinent cycle today. Whereas the configuration of Pangea during its break-up is well constrained due to the preservation of ocean floor from the Jurassic to the present (e.g., Seton et al. 2012), its amalgamation history is less certain and our only evidence is carved in the Paleozoic geological record. Controversy remains about the continental configuration of Pangea during its amalgamation (cf. Pangea A, B, C hypotheses; Domeier et al., 2012; Gallo et al., 2017; Belica et al., 2017), the number of participating continents and their kinematic evolution during the Paleozoic (e.g. Stampfli 2013; Domeier & Torsvik, 2014). Very importantly, there is a large and ongoing debate on when Pangea became a genuine supercontinent with contrasting age estimations ranging between 330 Ma to 240 Ma (e.g Veevers 2004; Blakey and Ranney, 2018).

The most important event in Pangea assemblage was the Late Paleozoic collision between Gondwana, Laurussia (Laurentia + Baltica + Avalonian terranes) and several microplates (Nance et al., 2010) resulting in the sinuous Variscan–Alleghanian orogen, which swirls several times from Bohemia to Alabama. Two of this orogenic curves are located in the Iberian Peninsula drawing an "S" shape: 1) the Cantabrian Orocline to the north, and 2) the Central Iberian curve to the south. In this paper we use the term orocline strictly in its kinematic definition: the curvature of an orocline is a product of vertical axis rotations (Johnston et al., 2013). The Cantabrian Orocline twists the Variscan trend from Brittany across the Bay of Biscay to enter into Central Iberia and its geometry is especially obvious in its core in NW Iberia (e.g. Weil et al., 2013). The Cantabrian Orocline formed by vertical axis rotations and is kinematically well constrained: it developed from Moscovian to Asselian times (~310–295 Ma.; e.g. Weil et al., 2010; Pastor-Galán et al., 2011). The geometry of the Central Iberian curve is, however, much less constrained due to limited exposures, being only obvious in the Morais Complex (W Iberia) and the Aragonese Branch of the Iberian Range (Fig. 1). From a kinematic point of view, the Central Iberian curve must have formed prior to 318 Ma (Pastor-Galán et al., 2016). It is not known, however, whether its formation involved vertical axis rotations and, if so, to what extent. The kinematics of the Cantabrian Orocline and the potentially expected vertical axis rotations in the Central Iberian curve require significant amounts of shortening and extension yet to be quantified and included in global reconstructions.

In this paper, we use paleomagnetism in the Santa Cruz de Nogueras Syncline (Aragonese Branch of the Iberian Range) to study the kinematic history and involvement of the Iberian Range in the Central Iberian curve. Our results allow, for the first time, to quantify the absolute minimum intracontinental deformation that Pangea underwent to accommodate the Late Carboniferous and Early Permian vertical axis rotations in the Variscan Belt.

2 Tectonic and geological settings

2.1 Tectonic and paleogeographic background

After the Late Silurian–Early Devonian collision between Avalonia s.l., Baltica and Laurentia had formed the Appalachian–Caledonide orogeny (e.g. Mac Niocaill, 2000; Domeier, 2016), the closure of the Rheic Ocean started (e.g. Nance et al., 2010). Subduction of the Rheic ocean was followed by the collision between Laurussia and Gondwana and several microplates, which formed the

Variscan–Alleghanian–Ouachita belt that seamed Pangea, at the end of the Carboniferous (e.g. Stampfli et al., 2013; Domeier and Torsvik, 2014).

Variscan deformation in Iberia commenced at ca. 400 Ma (e.g. Gómez Barreiro et al., 2006), although the first evidence of continental collision dates from ca. 365–370 Ma (e.g. Dallmeyer et al., 1997; López-Carmona et al., 2014) with the underplating of the Gondwanan margin below Laurussia. Deformation, metamorphism, magmatic episodes and syn-orogenic sedimentation migrated east-northeastward (in present-day coordinates) progressively towards the foreland (e.g. Dallmeyer et al., 1997) where deformation commenced at approximately 325 Ma. (e.g. Pérez-Estaún et al., 1991).

The Iberian Variscides depict a sinuous "S-shaped" geometry of two opposing first order magnitude bends (Fig. 1A) delineated by the well-known Cantabrian Orocline to the north and the Central Iberian curve to the south. Orogenic bends are classified based on the kinematics of their curvature development (e.g. Johnston et al., 2013). Correlations between changes in the structural grain and paleomagnetic directions or rock fabrics are evaluated using an orocline test (e.g. Pastor-Galán et al., 2017 and references therein), which distinguishes two end-members: 1) primary bends, showing a slope (m) = 0 and 2) secondary oroclines, with m=1. Intermediate relations ($0<m<1$) are known as progressive oroclines.

The Cantabrian Orocline (a.k.a. Cantabrian Arc and Cantabria-Asturias Arc) formed as a late orogenic feature in a short period of 10 to 15 Myr between 310 and 295 Ma (Pastor-Galán et al., 2011; Weil et al., 2013). Its structural trend traces a curvature that runs from Brittany across the Bay of Biscay passing through South England and Ireland into Central Iberia (Fig. 1A; Pastor-Galán et al., 2015a) and its geometry is evident from satellite imagery, especially at its core. Many paleomagnetic and geological studies support the Cantabrian Orocline as secondary feature (e.g. Weil et al., 2013 and references therein). Widespread mantle derived magmatism occurred coeval with the Cantabrian Orocline formation (between 310 and 290 Ma; Gutiérrez-Alonso et al., 2011a, b; Pastor-Galán et al., 2012a; Weil et al., 2013; Pereira et al., 2014).

Described for the first time by Staub (1926), the Central Iberian curve turns the Variscan orogen concave to the east immediately to the south of the Cantabrian Orocline (Fig. 1). In contrast with the Cantabrian Orocline, the geometry and kinematics of the Central Iberian curve are poorly understood and were overlooked for decades due to poor exposure (Martínez Catalán et al. 2015). The observations used in support of the Central Iberian curved geometry are: (i) paleocurrents recorded in Ordovician quartzites (Shaw et al., 2012); (ii) fold trends and inclusions in garnets (Aerden, 2004) and (iii) fold trends and aeromagnetic anomalies (Martínez-Catalán et al., 2012). Based on these arguments, three competing geometries have been proposed (Pastor-Galán et al., 2015b), which share two features in common: (1) the curvature encloses the center-west of Iberia with Galicia-Tras-os-Montes Zone in the core (Aerden, 2004; Pastor-Galán et al., in press b) and (2) the change in trend in the outer arc is primarily marked by the outcrops in the Aragonese Branch of the Iberian Range (Shaw et al., 2012).

Paleomagnetic results from the core and southern limb of the Central Iberian curve show an overall rotation that fits with the attitude of the southern limb of the Cantabrian Orocline (Pastor-Galán et al., 2015b; 2016; in press c). However, the timing constraints provided by these results established that no differential rotation occurred younger than ca. 318 Ma, and therefore, the available paleomagnetic data cannot refute a secondary nature for the arc, but it determines it to have occurred prior to 318 Ma (Pastor-Galán et al., in press c).

2.2 Geological Setting

The Variscan Orogen is classically divided into a number of tectonostratigraphic zones based on fundamental differences in their stratigraphic, structural, magmatic and metamorphic evolution (e.g. Ballevre et al., 2014). The Cantabrian Zone represents the foreland fold-and-thrust belt of the Variscan orogen. Structurally it is characterized by tectonic transport towards the core of the orocline, low finite strain values and locally developed cleavage (e.g. Pérez-Estaún et al., 1991; Kollmeier et al., 2000; Pastor-Galán et al., 2009). Illite crystallinity and conodont color alteration indexes are consistent with diagenetic conditions to very low-grade metamorphism (e.g. García-López et al., 2013; Pastor-Galán et al., 2013). The Cantabrian Zone is mostly preserved in NW Iberia in the core of the Cantabrian Orocline (Fig. 1A; Pastor-Galán et al., 2012b) but it also crops out in areas of the Aragonese Branch of the Iberian Range in E Iberia (Fig. 1B; Carls, 1983; 1988; Calvín-Ballester and Casas, 2014), where we performed our study (Figs. 1B and 2).

The Iberian Range (Fig. 1B) formed in response to the intraplate deformation triggered by the Alpine orogeny in the eastern central part of the Iberian Peninsula during the Cenozoic (e.g. Álvaro et al., 1978; Cortés-Gracia and Casas-Sainz, 1996; Casas-Sainz and Faccena, 2001). It is configured in two main branches trending mainly NW-SE: the Aragonese Branch (northwards) and the Castilian Branch (southwards). Our study focuses on the central part of the northernmost Aragonese Branch, where two elongated Paleozoic units, separated by the Cenozoic Calatayud basin, crop out. Paleozoic rocks in the studied area are structured into two tectonostratigraphic units: Badules and Herrera. Whereas the Herrera unit is the continuation of the foreland (Cantabrian Zone), the Badules unit represents more internal zones of the orogen (e.g. Gozalo and Liñán, 1988). The Herrera Unit preserves over 9000 m-thick sedimentary sequence containing a Cambrian-Silurian alternation of sandstones and shales and, over it, an Upper Silurian–Devonian series of shales (Luesma, Nogueras and Mariposas Fms.), sandstones and limestones (Calvín-Ballester and Casas, 2014 and references therein) which crop out at the south of the unit (Figs. 1B and 2). The Herrera unit is characterized by an imbricate thrust system with a foreland-dipping geometry in which the deformation and cleavage diminishes eastwards (Calvín et al., 2014). Silurian to Devonian rocks crop out in two overturned synclines with NNW–SSE to NW–SE trend (Fig. 2): Santa Cruz and Loscos synclines. During Early Permian mantle derived magmatism affected the Herrera unit and the igneous rocks happen as effusive, subvolcanic dykes and sills and minor plutons (e.g. Calvín et al., 2014 and references therein). Around 1500 m-thick series of Mesozoic rocks (Calvín et al.,

2014) overlay the Paleozoic units. Both sequences underwent gentle folding during the Alpine compression with no associated penetrative structures (Cortés-Gracia and Casas-Sainz, 1996).

The present outcrop of Paleozoic basement rocks in the Iberian Range is strongly conditioned by subsequent Late Paleozoic-Mesozoic rifting episodes, the later inversion of those basins during the Alpine deformation in Cenozoic times and a final extensional event during the Neogene (Salas and Casas, 1993). Two major rifting events took place during Late Permian-Triassic and during Late Jurassic-Early Cretaceous controlled by major Variscan anisotropies and main depocenters were located NW and SE of the study area. Subsequent Alpine deformation inverted the previous extensional basins and produced a geometrically complicated fold and thrust belt displaying interference geometries, strike and reverse-slip movements and complex thin-skinned thick-skinned relationships (Salas et al., 2001; Guimerá et al., 2004; De Vicente et al., 2009; Izquierdo-Llavall et al., 2018). Finally, a Neogene NW-SE extension related to the opening of the Mediterranean western basins led to the final configuration of the system (Simón, 1983; Roca y Guimerà, 1992).

Previous paleomagnetic studies in Permian and Mesozoic rocks in the region have reported primary Oxfordian and Permian components (Juárez et al., 1994 and Calvin et al., 2014 respectively) as well as Lower Cretaceous remagnetizations (Juárez et al., 1998; Gong et al., 2008). However, reported declinations of all these results should be used with caution since recent data from younger Mesozoic and Cenozoic units confirmed the occurrence of clockwise rotations (CW) related to Alpine compression (Mauritsch et al., 2018). Following these authors, the mean Cenozoic paleomagnetic direction in the Central Iberian Range was Dec./Inc. = 025˚/57˚ (k = 35.4) which yields a consistent 21° CW rotation respect to the Cenozoic reference direction for Iberia (Dec./Inc. = 004˚/46˚; k = 110.6). In addition, the paleomagnetic results are supported by shortening differences along-strike found after the restoration of balanced cross sections in the region (Izquierdo-Llavall et al., 2018).

3 Methods and Results

We drilled a total of 300 cores from 28 sites with a petrol engine drill and took over 100 structural orientations (Fig. 2; Table 1; Supplementary File SF1 for exact location) in the Silurian and Devonian rocks that crop out to the south of the Herrera unit at the Aragonese Branch of the Iberian Range (Figs. 1 and 2). We performed all analyses at Paleomagnetic Laboratory Fort Hoofddijk, Universiteit Utrecht, The Netherlands.

3.1 Structure and anisotropy of the magnetic susceptibility

The Santa Cruz Syncline is a close to recumbent cylindrical fold with a non-plunging axis that swings from NW-SE to N-S trend (Fig. 2A). In the studied area little to no penetrative fabrics developed and strain patterns based on field constraints are limited to thrusts and folds.

Anisotropy of magnetic susceptibility (AMS) is a very sensitive method that can help describing deformational events even in weakly deformed contexts where tectonic lineation and foliation have not developed (e.g. Mattei et al., 1997; Weil and Yonkee, 2009; Parés, 2015) and it is represented graphically as an ellipsoid whose principal axes are $k_{max} > k_{int} > k_{min}$ (Borradaile, 1988: Parés, 2015 and references therein). The shape of the AMS ellipsoid depends on the crystallographic preferred orientation of the individual components, its compositional layering, distribution and size of microfractures and the shape, size and preferred orientation of mineral grains (e.g. Butler, 1992; Tarling and Hrouda, 1993; Tauxe, 2010). In undeformed sedimentary rocks, AMS ellipsoid usually shows an oblate geometry with its foliation plane parallel to bedding and k_{min} perpendicular to it (e.g. Tarling and Hrouda, 1993). In contrast, the AMS ellipsoid in deformed rocks develops a magnetic lineation (k_{max}) typically representing intersection lineations in weakly deformed settings (i.e. parallel to fold axis; e.g. Oliva-Urcia et al., 2009) or maximum extension directions (e.g. Cifelli et al., 2005; García-Lasanta et al., 2015). In strongly deformed areas, the AMS ellipsoid becomes oblate again, this time with k_{min} parallel to the tectonic foliation (e.g. Weil and Yonkee, 2009).

We measured the AMS of 162 samples from our Santa Cruz syncline collection with an AGICO MFK1-FA susceptometer. Samples from sites MD1 to MD7, MD26 and MD27 yielded no interpretable AMS results (Supplementary File SF2). The rest of the samples show triaxial AMS ellipsoids (Fig. 2B and Supplementary File SF2) but close to oblate where the most developed fabrics show k_{min} perpendicular to bedding. Although k_{int} and k_{max} are similar they are distinctly different, magnetic lineation (k_{max}) is roughly oriented to the NNE-SSW with little to no plunge and coinciding with the fold axis trend (Fig. 2A), whereas k_{int} is mostly parallel to the shortening direction (perpendicular to the fold axis). All these results confirm the weak deformation underwent by the studied rocks.

3.2 Paleomagnetism

We used both thermal and alternating field (AF) demagnetizations to investigate the magnetic remanence of the collected samples. AF demagnetization was carried out using a robotic 2G-SQUID magnetometer available at Utrecht University, through variable field increments (4–10 mT) up to 70–100 mT. In those samples where high-coercivity, low-blocking temperature minerals (e.g. goethite, maghemite) were expected, a pre-heating to 150 °C was coupled to AF demagnetization (van Velzen and Zijderveld, 1995). Stepwise thermal demagnetization was carried in the remaining samples through 20–100 °C increments up to complete demagnetization (Fig. 3; Supplementary File SF3). Principal component analysis (PCA; Kirschvink, 1980) was used to isolate the direction of the characteristic remanent magnetization and results were represented by orthogonal vector end-point demagnetization diagrams (Zijderveld, 1967) using Paleomagnetism.org (Koymans et al., 2016). Representative Zijderveld diagrams are shown in Fig. 3. A minimum of 5 steps was considered to characterize a remanent component. In ~35 samples, two components appear to overlap; for such cases we applied the method of demagnetization great circles (Fig. 3). We used the approach of McFadden and McElhinny (1988) in combining great circles and linear best fits (set points).

Given the structural coherence between the studied sites and the robust paleomagnetic signal of the samples we combined all the results in a single locality. From the PCA analysis we could separate several components to which we applied a fixed 45° cut-off to their VGP distributions (Deenen et al., 2011). Mean directions (Table 1) were evaluated using Fisher statistics (1953) of virtual geomagnetic poles (VGPs) corresponding to the isolated magnetic directions, following Deenen et al. (2011). All statistics were performed with www.paleomagnetism.org (Koymans et al., 2016) and VPD software (Ramón et al., 2017). Most samples show a component which is removed at low temperatures and low coercivities (100–180 °C or 10-12 mT; Fig. 3 and Supplementary material). We consider this component as a viscous remanent magnetization (VRM), because of its similarity to the recent field.

In addition to the VRM, we have identified 3 components showing distinctive components:

Component P: samples from Early Permian dykes and sills show a single polarity component with southwards declination and very shallow inclination (Dec./Inc. = 191.3˚/-8.8˚; k = 35.3, α_{95} = 4.4, K = 55.5, A_{95} = 3.5; Fig. 4; Table 1), which is consistent with that described in similar rocks in the area (Calvín et al., 2014). Component P is predominant in most of the sedimentary Devonian rocks studied (104 specimens) with a slightly different average of Dec./Inc. = 183.2˚/4.5˚ (k = 17.6, α_{95} = 3.4˚, K = 35.8, A_{95} = 2.3˚; Table 1; Fig. 4) and a larger dispersion ($K_{sedimentary}$=35.8 vs. $K_{igneous}$=55.5, Table 1). This component clusters better before any tilt correction (Table 1). When occurring together with other components, it is usually removed at 300-350˚ degrees (lower T component) and over 40-50 mT (higher coercivity component). The average direction of all the samples (igneous and sedimentary) combined is Dec./Inc. = 185.1˚/1.4˚ (k = 17.8, α_{95} = 3˚, K = 34.8, A_{95} = 2.1˚; Table 1).

Component #1: In 49 specimens from Devonian sedimentary rocks, we identified a single polarity component heading southeast with shallow inclinations and an average direction Dec./Inc. =

150.4˚/8.3˚ (k = 15.5, α_{95} = 5.3˚, K = 29, A95 = 3.8˚; Fig. 5; Table 1). This component does not pass a fold test (Fig. 5B; Tauxe and Watson, 1994).

Component #2: 46 specimens from the Devonian sedimentary samples show a two polarity component that clusters significantly better after structural correction and passes a fold test (Fig. 6; Tauxe and Watson, 1994). Both polarities share a common distribution following the coordinate bootstrap test of Tauxe et al. (2010) (Fig. 6). This component trends eastwards and shows shallow inclinations, slightly higher than in Component #1 (average Dec./Inc. = 107.3˚/12.7˚; k = 8, α_{95} = 7.9, K = 13, A_{95} = 6.1˚) (Table 1).

Demagnetization analyses and thermomagnetic runs (Supplementary Files SF3 and SF4 respectively) indicate that the principal magnetic carrier in dykes and sills is (Ti-poor) magnetite, as evidenced by unblocking temperatures between 480 and 580˚C and alternating magnetic fields peaks of 40-60 mT. Results from limestones and sandstones also point to (Ti-poor) magnetite as the main carrier of the NRM, evidenced by maximum unblocking temperatures of 400–580 °C and alternating magnetic fields of 60–90 mT (Fig. 3). The main magnetic carrier of the red limestones is hematite, demagnetizing over 600 °C and largely resistant to AF demagnetization. Some limestones show a relatively large goethite component that was fully removed at 100˚C.

4 Discussion

Unraveling the kinematics and deformational mechanisms of areas that underwent several tectonic events is a complex task that has to be solved backwards in time, especially when dealing with vertical axis rotations (Pueyo et al., 2016): it is impossible to solve accurately the oldest movements without solving the youngest ones. Several authors described Alpine tectonics involving the basement units in the Iberian Range (e.g. Izquierdo-Llavall et al., 2018). Despite the vertical axis rotations described in the area (e.g. Mauritsch et al., 2018), the Santa Cruz Syncline shows a sub-horizonal axis (Fig. 2A) and the Mesozoic and Paleozoic rocks overlying the Santa Cruz Syncline show sub-horizontal dips and no signs of refolding, thrusting, major tilting nor penetrative internal deformation. These data support that the particular area around the Santa Cruz Syncline did not record any significant Alpine tilting.

AMS ellipsoids fit with the macrostructural data (Fig. 2A and B). The k_{min} axes are perpendicular to the bedding plane, caused by compaction after sedimentation. Despite maximum and intermediate magnetic axes distributions show a rather large dispersion, they arrange around an orientation maximum, suggesting a tectonic fabric superimposed on the sedimentary fabric. The magnetic lineation (k_{max} distribution) is parallel to the Santa Cruz syncline's fold axis or, equivalently, perpendicular to the shortening direction. The structural trend (dominant N-S) as well as the overturned feature of the analyzed structures (particularly the Santa Cruz de Nogueras syncline) strongly differs from the expected Alpine grain (NW-SE). The AMS response and its consistency with the general macrostructure support that Variscan deformation was not intense and did not trigger noticeable internal deformation in the studied lithologies. Hence and apart from rigid-body passive movements, post-Permian deformation is negligible. Absence of major internal deformation events simplifies the interpretation of Paleozoic paleomagnetic directions.

4.1 Paleomagnetism

We have identified three different magnetic components. They may occur individually or in couples (Fig. 3), regardless of their lithology or structural position.

Component P

All Lower Permian and many of the sites sampled in Siluro-Devonian sedimentary rocks, yielded a single polarity component which clusters better before any correction, with declinations consistently to the south and equatorial paleolatitudes (Fig. 4; Table 1). This indicates that the magnetization must have been acquired when Iberia was situated at equatorial latitudes during a long-lasting reverse chron, since no polarity changes have been found. We know that Iberia crossed the equator from the southern to northern hemisphere during the Early Permian (Osete et al., 1997; Weil et al., 2010) and migrated, together with Pangea, rapidly towards the north (Torsvik et al., 2012). We suggest the Component P to be acquired at Early Permian times during the Permo-Carboniferous Reversed Superchron (PCRS) ranging 314-265 Ma (Langereis et al., 2010). Therefore, this magnetization is likely primary for the Early Permian mafic dykes and sills that intruded and subsequently overprinted the Devonian sedimentary sequence. There is a small but significant difference in inclination between the remagnetized vector in the sedimentary rocks (4.5 ± 4.7˚) and the potentially primary magnetization found in the dykes/sills (-8.8 ± 6.9˚). This divergence may indicate that rocks were magnetized at slightly different times, with the overprint being an earlier magnetization, perhaps fluid-driven, when Iberia was still in the southern hemisphere. Calvín et al. (2014) described a very similar component in Early Permian intrusions in an equivalent area of the Iberian Range.

Component P shows inclinations very similar to the Component eP for stable Iberia of Weil et al. (2010), but it is rotated ~22˚ CW with respect to eP. This rotation coincides with the rotation recorded by the Cenozoic and Mesozoic rocks of the Aragonese Branch of the Iberian Range (21˚ CW following Mauritsch et al., 2018) during the Alpine orogeny. We conclude that the only post-Permian event that the studied Paleozoic rocks recorded is a ~22˚ CW vertical axis rigid-body rotation together with Mesozoic and Cenozoic rocks possibly related to Alpine basement thrusting that underwent differential displacement along-strike during its movement (Izquierdo-Llavall et al., 2018).

Component #1

Component #1 is a single polarity reverse component that does not pass a fold test (Fig. 5). It concerns a shallow component from the southern hemisphere (Dec./Inc. = 150.4˚/8.3˚; Table 1). The magnetization of this component must therefore have been acquired before Iberia crossed the equator in the Early Permian (Weil et al., 2010) but after the onset of the PCRS (~314 Ma), constraining Component #1 to be a Late Carboniferous overprint. If we correct for the ~22˚ CW Cenozoic rotation, this component shows a ~25˚ CCW rotation with respect to the Early Permian pole for stable Iberia (Weil et al., 2010). A CCW rotation during the latest Carboniferous is consistent with the Cantabrian Orocline sense and timing of rotation (e.g. Weil et al., 2013). Considering the strike of the Iberian range, however, the expected magnitude of rotation would be higher. For this reason, we consider Component #1 to be a Late Carboniferous overprint that occurred at the latest stages of Cantabrian Orocline formation.

Component #2

We identified Component #2 in 46 specimens from different sites within the Santa Cruz Syncline (Supplementary File SF3). Component #2 passes the fold test and shows both normal and reverse polarity distributions that pass a reversal test (Fig. 6). The two positive field tests would support a (pseudo)primary magnetization (e.g. Van der Voo, 1990). However, the scarce available paleomagnetic data for Siluro-Devonian times indicate that the northern margin of Gondwana and the derived terranes were at latitudes of 30-40˚ S (Hasma et al., 2015; Torsvik et al., 2012). More importantly, biostratigraphic and faunal constraints from the Santa Cruz syncline support a medium latitude (~23˚ to ~66˚) formation for the sampled units (Carls, 1988; Villas, 1995). Therefore, the inclinations found (12.7˚ ± 11.7˚) are too shallow when compared to the geological constraints, indicating a magnetization acquired when the rocks were at equatorial paleolatitudes (λ = 6.4˚ S ± ~6˚). Following the global apparent polar wander path (GAPWaP) of Torsvik et al. (2012) calculated for Iberia (given in Koymans et al., 2016) such low paleolatitude (6.4˚ S) would only be expected for Iberia in Middle-Late Carboniferous times, during the Variscan Orogeny. The Variscan Orogeny produced pervasive remagnetizations in Iberia (e.g. Weil et al., 2013: Pastor-Galán et al., in press c). Therefore, we suggest a Late Mississippian-Early Pennsylvanian (Middle Carboniferous) secondary origin for Component #2. The remagnetization likely occurred just before the onset of the long-lasting PCRS (ca. 314 Ma) allowing the occurrence of two polarities.

4.2 On the Central Iberian bend and extent of the Cantabrian Orocline

Our new paleomagnetic results show a vertical axis rotation of ~22˚ CW of the Early Permian Component P (Fig. 7) with respect to stable Iberia at that time (Weil et al., 2010). This 22˚ rotation is identical to the rotation observed in covering Mesozoic and Cenozoic rocks in the area

(Mauritsch et al., 2018). Our results also establish a differential pre-Permian CCW rotation recorded by Components #1 (~35˚) and #2 (~80˚) with respect to Component P. Component #1 shows a CCW rotation of less magnitude (~25˚) and, like P, only reverse polarity. We interpret Component #1 as an overprint occurring during the Cantabrian Orocline formation, some time between ~310 Ma and 295 Ma (Pastor-Galán et al., 2015b; in press c). This interpretation explains the similar inclination, declination and single polarity (Fig. 7). The change in structural trend in the Paleozoic rocks of the Iberian Range corresponds roughly to 25˚ (Fig. 7). We have calculated a rotation of 22° around an Euler pole located where the strike of the orogen changes in the Iberian Range (42˚N, 2.4W) and the results coincide with the Iberian APWP for the Late Carboniferous (Pastor-Galán et al. 2016) (Fig. 7). After restoring the 22˚ CW Cenozoic rotation, the structural trend of the Paleozoic outcrops of the Aragonese Branch of the Iberian Range become near parallel to the orogen strike in the southern limb of the Cantabrian Orocline (Figs. 1 and Fig. 7).When accounting for the 22˚ CW, Component #2 shares a common distribution (following the coordinate bootstrap test of Tauxe et al. 2010) with the Late Mississippian-Early Pennsylvanian pole of Iberia calculated by Pastor-Galán et al. (2016) (Supplementary File SF5).

Once the structure and the paleomagnetic results are restored to a pre-alpine rotation, the Component #2 can be compared with the orocline test of the Cantabrian Zone. We have plotted Component #2 into the Bootstrapped Orocline Test for the Cantabrian Orocline (Pastor-Galán et al., 2017) obtaining a perfect fit (Fig. 7C). Thus, Component #2 shows the paleolatitude and CCW rotation at 320 Ma (Figs. 7 and 8) expected at the southern limb of the Cantabrian Orocline. Our data indicate that most of the Iberian Massif rotated ~70˚ CCW with the exception of the very North (at present day coordinates) where the hinge of the Cantabrian Orocline is located (Fig. 1). Therefore, the extent of the vertical axis rotations associated with the Cantabrian Orocline formation is much larger than originally hypothesized.

Our results show that the change in trend in the Aragonese Branch of the Iberian Range has a Cenozoic (Alpine) rather than a Paleozoic (Variscan) origin. With the new data presented in this paper, we rule out the idea of the Central Iberian curve as a large Late Variscan orocline coupled to the Cantabrian Orocline. We claim the geometry of the Iberian bend is the results of a combination of processes. The curvature of the inner arc (Morais Complex; Fig. 1) is the result of a pre- 318 Ma process, probably during the early stages of collision and involving no vertical axis rotations (Pastor-Galán et al., 2016). The outer arc curvature, however, is the result of much younger Alpine tectonics: these are commonly disregarded in studies of the Variscan Orogen of Iberia.

4.3. Quantifying Pangea's intraplate deformation

We reconstruct the Iberian plate following the Cantabrian Orocline based on the global reconstruction of Domeier and Torsvik (2014), in order to quantify the minimum deformation accommodated in the core of Pangea and using Gplates (Boyden et al., 2011). Our reconstruction assumes that most of present day Iberia behaved rigidly, despite the evidence of crustal deformation in the core of the Cantabrian Orocline (e.g. Pastor-Galán et al., 2012b; Merino-Tomé et al., 2009). We also assume a rigid Pangea. The reconstruction shows a fixed Pangea. We proceed that way since: 1) Gplates has limited possibilities to account for block deformation, and 2) it is uncertain where and to what extent the Cantabrian Orocline buckling affected other continental blocks (Pastor-Galán et al., 2015a). To minimize the effect of the Cantabrian Orocline formation, we avoided Iberia overlapping with other continental blocks during the rotation and we did not consider Corsica, Sardinia and Balearic as part of the southern limb of the orocline. Therefore, our reconstruction can only provide the minimum amount of convergence and extension provided by a coherent movement for Iberia.

We tested our reconstruction using paleomagnetic constraints. For this, we applied an iterative approach, in which we determined total Euler reconstruction poles from 315-285 Ma of the Iberian block relative to Pangea using recent published data (Pastor-Galán et al., 2016; in press c and this study). We also modified the calculated Euler poles in Domeier and Torsvik (2014) from the period 285-200 Ma using the databases from Dinarès et al., 2005 and Vissers et al., 2016 (Fig. 8; Table 2). Then, we tested our Euler rotations to predict the Global Apparent Polar Wander Path in the coordinates of Iberia (Table 2). We then iteratively updated our reconstruction until the paleomagnetic data overlap with the polar wander paths as predicted by the reconstruction (Figure 9).

Our reconstruction shows that, to fulfill the paleomagnetic constraints, a minimum of ~1000 km of convergence must have been accommodated south of present day France and ~1000 km of extension divided between the east (~600 km) and south (~400 km) of the Iberian block (Fig. 9). To accommodate these minimum amounts of convergence and extension we require the development of large basins and at least one subduction zone (either oceanic or intracontinental). Although those features are yet to be described, the Iberian Peninsula was extensively intruded by mantle derived rocks during that particular time interval (e.g. Gutiérrez-Alonso et al., 2011a; Pereira et al., 2014). The mantle character of the intrusions (Perini et al., 2004; Gutiérrez-Alonso et al., 2011b) suggests an origin linked to lithospheric foundering (e.g. subduction slab break-off, delamination…). In addition, those intrusions affected both hinterland and foreland indicating that the process happened in a location different from the sutures related with the collision between Gondwana and Laurussia (Weil et al., 2013; Pereira et al., 2014).

There is an ongoing debate on how and when Pangea became a rigid supercontinent (e.g. Gallo et al., 2017) with contrasting age estimations ranging between 330 Ma to 240 Ma (e.g Veevers 2002; Blakey and Ranney, 2017). The quantification, for the first time, of a minimum of 1000 km of convergence accommodated in the core of Pangea due to the Cantabrian Orocline formation in the Late Carboniferous indicates that Pangea did not behave as a rigid superplate at least until 290 Ma.

5 Conclusions

Our paleomagnetic and structural results from the Santa Cruz syncline (Aragonese Branch of the Iberian Range) show a vertical axis rotation of ~22˚ clockwise (CW) during the Cenozoic and about 70˚ counterclockwise (CCW) during the Late Carboniferous. Once the Cenozoic rotation is accounted for, the structural and paleomagnetic trends of the Aragonese Branch become parallel to those in the southern limb of the Cantabrian Orocline, ruling out a Variscan origin for the outer Central Iberian curve. Thus, the Central Iberian curve is an accident product of a combination of processes: 1) an Early Variscan non-rotational process in its core and 2) a Cenozoic CW rotation in its outer arc. In addition, the fit of the Aragonese Branch of the Iberian Range with the Cantabrian Zone indicates that most of the Iberian Massif rotated ~70˚ CCW with the exception of its hinge (located at the NW of the Iberian Peninsula). This means that the extent of the vertical axis rotations associated to the Cantabrian Orocline formation is much larger than previously thought. Using the most recent paleomagnetic constraints and Gplates (Boyden et al., 2011), we have quantified in 1000 km the minimum amount of convergence in the core of Pangea required to accommodate the rotations in Iberia associated with the Cantabrian Orocline.

Acknowledgements

We thank Enrique Villas and Andrés Pocoví for field assistance and friendship. DPG is funded by a Japan Society for Promotion of Science (JSPS) fellowship for overseas researchers (P16329), a MEXT/JSPS KAKENHI Grant (JP16F16329) and ELP and CGL are financed by CGL2014-54118. DPG wants to thank Thomas Earl Petty, you dropped me in free fallin’ and now I’m learning to fly. All data can be accessed from DPG’s Github public repository. This paper is part of UNESCO IGCP Projects 574: Buckling and Bent Orogens, and Continental Ribbons; 597: Amalgamation and breakup of Pangaea: The Type Example of the Supercontinent Cycle; and 648: Supercontinent Cycles and Global Geodynamics.

References

Aerden, D. (2004). Correlating deformation in Variscan NW-Iberia using porphyroblasts; implications for the Ibero-Armorican Arc. *Journal of Structural Geology*, *26*(1), 177–196.

Alvaro M, Capote R, Vegas R. Un modelo de evolución geotectónica para la Cadena Celtibérica. Acta Geológica Hispánica, 1978; 14: 172–177.

Ballèvre, M., Martinez Catalan, J. R., Lopez-Carmona, a., Pitra, P., Abati, J., Fernandez, R. D., … Sanchez Martinez, S. (2014). Correlation of the nappe stack in the Ibero-Armorican arc across the Bay of Biscay: a joint French-Spanish project. *Geological Society, London, Special Publications*, 77–113. https://doi.org/10.1144/SP405.13

Barreiro, J. G., Wijbrans, J. R., Castineiras, P., Catalan, J. R. M., Arenas, R., Garcia, F. D., & Abati, J. (2006). Ar-40/Ar-39 laserprobe dating of mylonitic fabrics in a polyorogenic terrane of NW Iberia. *Journal of the Geological Society*, *163*, 61–73.

Belica, M. E., Tohver, E., Pisarevsky, S. A., Jourdan, F., Denyszyn, S., & George, A. D. (2017). Middle Permian paleomagnetism of the Sydney Basin, Eastern Gondwana: Testing Pangea models and the timing of the end of the Kiaman Reverse Superchron. *Tectonophysics*, *699*, 178–198. https://doi.org/10.1016/J.TECTO.2016.12.029

Blakey, R. C., & Ranney, W. D. (2018). The Amalgamation of Pangaea and the Sonoma Orogeny: Early Permian to Early Triassic – Ca. 300–240 Ma. In *Ancient Landscapes of Western North America* (pp. 83–88). Cham: Springer International Publishing. https://doi.org/10.1007/978-3-319-59636-5_6

Borradaile, G. J. (1988). Magnetic susceptibility, petrofabrics and strain. *Tectonophysics*, *156*(1–2), 1–20. https://doi.org/10.1016/0040-1951(88)90279-X

Boyden, J.A., Müller, R.D., Gurnis, M., Torsvik, T.H., Clark, J.A., Turner, M., Ivey-Law, H., Watson, R.J., Cannon, J.S., 2011. Next-generation plate-tectonic reconstructions using GPlates. In: Keller, G.R., Baru, C. (Eds.), Geoinformatics: Cyberinfrastructure for the Solid Earth Sciences. Cambridge University Press, pp. 95–113.

Butler, R.F., 1992. Paleomagnetism: magnetic domains to geologic terranes (Vol. 319). Boston: Blackwell Scientific Publications.

Calvín-Ballester, P., Casas-Sainz, A.M., 2014. Folded Variscan thrust in the Herrera Unit of the Iberian Range (NE Spain). In: Bastida, F., Llana-Fúnez, S., Marcos, A. (eds.). Deformation Structures and Processes within the Continental Crust. London, Geological Society, 394 (Special Publications), 39-52.

Calvin, P., Casas, A.M., Villalaín, J. J., & Tierz, P. (2014). Reverse magnetic anomaly controlled by Permian Igneous rocks in the Iberian Chain (N Spain). *Geologica Acta*, *12*(3), 193–207. https://doi.org/10.1344/GeologicaActa2014.12.3.2

Carls, P., 1983. La Zona Asturoccidental-Leonesa en Aragón y el Macizo del Ebro como prolongación del Macizo Cantábrico. Libro Jubilar J. M. Ríos. Instituto Geológico y Minero de España, 3, 11-32.

Carls, P., 1988. The Devonian of Celtiberia (Spain) and Devonian paleogeography of SW Europe." In Devonian of the World Edited by: N.J. McMillan, A.F. Embry, D.J. Class. Canadian Society of Petroleum Geologist, Memoir 14 (1), 421-466.

Carls, P., & Valenzuela-Ríos, J. I. (2002). Devonian-Carboniferous rocks from the Iberian Cordillera. In: Palaeozoic Conodonts from Northern Spain. Edited by: García-López S, Bastida F. Instituto Geológico y Minero de España, Serie Cuadernos del Museo Geominero. p. 299–314

Casas-Sainz, A.M. Faccena, C. (2001). Tertiary compressional deformation of the Iberian plate. *Terra Nova*, *13*(4), 281-288.

Cifelli, F., Mattei, M., Chadima, M., Hirt, A.M., Hansen, A. (2005). The origin of tectonic lineation in extensional basins: Combined neutron texture and magnetic analyses on ‘undeformed’ clays. *Earth and Planetary Science Letters*, 235, 62–78. https://doi.org/10.1016/j.epsl.2005.02.042

Cole, S. R., Ausich, W. I., Colmenar, J., & Zamora, S. (2017). Filling the Gondwanan gap: paleobiogeographic implications of new crinoids from the Castillejo and Fombuena formations (Middle and Upper Ordovician, Iberian Chains, Spain). *Journal of Paleontology*, 1-20.

Cortes Gracia, A.L. and Casas-Sáinz, A.M., 1996. Deformación alpina de zócalo y cobertera en el borde norte de la Cordillera Ibèrica (Cubeta de Azuara-Sierra de Herrera). Revista de la Sociedad Geológica de España, 9(1), pp.51-66.

Gozalo, R. and Liñan, E., 1988. Los materiales hercínicos de la Cordillera Ibérica en el contexto del Macizo Ibérico. Estudios geológicos, 44(5-6), pp.399-404.

Dallmeyer, R. D., Catalán, J. R. M., Arenas, R., Gil Ibarguchi, J. I., Gutiérrez^Alonso, G., Farias, P., … Aller, J. (1997). Diachronous Variscan tectonothermal activity in the NW Iberian Massif: Evidence from 40Ar/39Ar dating of regional fabrics. *Tectonophysics*, *277*(4), 307–337. https://doi.org/10.1016/S0040-1951(97)00035-8

Deenen, M.H.L., Langereis,, C.G., Van Hinsbergen, D.J.J. and Biggin, A.J. (2011). Geomagnetic secular variation and the statistics of palaeomagnetic directions, *Geophysical Journal International*, *186*, 509-520.

Dinarès-Turell, J., Diez, J. B., Rey, D., & Arnal, I. (2005). “Buntsandstein” magnetostratigraphy and biostratigraphic reappraisal from eastern Iberia: Early and Middle Triassic stage boundary definitions through correlation to Tethyan sections. *Palaeogeography, Palaeoclimatology, Palaeoecology*, *229*(1–2), 158–177. https://doi.org/10.1016/J.PALAEO.2005.06.036

De Vicente, G., Vegas, R., Muñoz-Martín, A., Van Wees, J. D., Casas-Sáinz, A.M., Sopeña, A., Fernández-Lozano, J., 2009. Oblique strain partitioning and transpression on an inverted rift: The Castilian Branch of the Iberian Chain. Tectonophysics, 470, 224-242.

Domeier, M. (2016). A plate tectonic scenario for the Iapetus and Rheic Oceans. *Gondwana Research*, *36*, 275–295.

Domeier, M., Van Der Voo, R., & Torsvik, T. H. (2012). Paleomagnetism and Pangea: The road to reconciliation. *Tectonophysics*, *514–517*, 14–43. https://doi.org/10.1016/j.tecto.2011.10.021

Fisher, R. (1953). Dispersion on a Sphere. *Proceedings of the Royal Society A: Mathematical, Physical and Engineering Sciences*, *217*(1130), 295–305. https://doi.org/10.1098/rspa.1953.0064

Gallo, L. C., Tomezzoli, R. N., & Cristallini, E. O. (2017). A pure dipole analysis of the Gondwana apparent polar wander path: Paleogeographic implications in the evolution of Pangea. *Geochemistry, Geophysics, Geosystems*, *18*(4), 1499–1519. https://doi.org/10.1002/2016GC006692

García-Lasanta, C., Oliva-Urcia, B., Román-Berdiel, T., Casas, A. M., Gil-Peña, I., Sánchez-Moya, Y., Sopeña, A., Hirt, A. M., Mattei, M. (2015). Evidence for the Permo-Triassic transtensional rifting in the Iberian Range (NE Spain) according to magnetic fabrics results. *Tectonophysics*, *651*, 216–231. https://doi.org/10.1016/j.tecto.2015.03.023

García-Lasanta, C., Casas Sainz, A., Villalaín, J. J., Oliva-Urcia, B., Speranza, F., Mochales, T. (2017). Remagnetizations used to unravel large.scale fold kinematics: a case study in the Cameros basin (N Spain). *Tectonics*, *36(4)*, 714–729. https://doi.org/10.1002/2016TC004459

García-López, S., Bastida, F., Aller, J., Sanz-López, J., Marín, J. A., & Blanco-Ferrera, S. (2013). Tectonothermal evolution of a major thrust system: The esla-valsurbio unit (cantabrian Zone, NW Spain). *Geological Magazine*, *150*(6), 1047–1061. https://doi.org/10.1017/S0016756813000071

Guimerà, J., Mas, R., Alonso, Á., 2004. Intraplate deformation in the NW Iberian Chain: Mesozoic extension and Tertiary contractional inversion. Journal of the Geological Society, 161, 291-303.

Gutiérrez-Alonso, G., Fernández-Suárez, J., Jeffries, T. E., Johnston, S. T., Pastor-Galán, D., Murphy, J. B., … Gonzalo, J. C. (2011). Diachronous post-orogenic magmatism within a developing orocline in Iberia, European Variscides. *Tectonics*, *30*(5). https://doi.org/10.1029/2010TC002845

Gutiérrez-Alonso, G., Murphy, J. B., Fernández-Suárez, J., Weil, A. B., Franco, M. P., & Gonzalo, J. C. (2011). Lithospheric delamination in the core of Pangea: Sm-Nd insights from the Iberian mantle. *Geology*, *39*(2), 155–158. https://doi.org/10.1130/G31468.1

Hansma, J., Tohver, E., Yan, M., Trinajstic, K., Roelofs, B., Peek, S., Slotznick, S.P., Kirschvink, J., Playton, T., Haines, P. and Hocking, R., 2015. Late Devonian carbonate magnetostratigraphy from the Oscar and Horse Spring Ranges, Lennard Shelf, Canning Basin, Western Australia. Earth and Planetary Science Letters, 409, pp.232-242.

Johnston, S. T., & Weil, A. B. (2013). Oroclines : Thick and thin Oroclines : Thick and thin, (February). https://doi.org/10.1130/B30765.1

Juárez, M. ., Lowrie, W., Osete, M. ., & Meléndez, G. (1998). Evidence of widespread Cretaceous remagnetisation in the Iberian Range and its relation with the rotation of Iberia. Earth and Planetary Science Letters, 160(3–4), 729–743. https://doi.org/10.1016/S0012-821X(98)00124-1

Juárez, M. T., Osete, M. L., Meléndez, G., Langereis, C. G., & Zijderveld, J. D. A. (1994). Oxfordian magnetostratigraphy of the Aguilón and Tosos sections (Iberian Range, Spain) and evidence of a pre-Oligocene overprint. Physics of the Earth and Planetary Interiors, 85(1–2), 195–211. https://doi.org/10.1016/0031-9201(94)90017-5

Kirschvink, J. L. (1980). The least-squares line and plane and the analysis of palaeomagnetic data. Geophysical Journal International, 62(3), 699–718. https://doi.org/10.1111/j.1365-246X.1980.tb02601.x

Kollmeier, J. M., van der Pluijm, B. A., & Van der Voo, R. (2000). Analysis of Variscan dynamics; early bending of the Cantabria-Asturias Arc, northern spain. Earth and Planetary Science Letters, 181(1–2), 203–216.

Koymans, M. R., Langereis, C. G., Pastor-Galán, D., & van Hinsbergen, D. J. J. (2016). Paleomagnetism.org: An online multi-platform open source environment for paleomagnetic data analysis. Computers and Geosciences, 93. https://doi.org/10.1016/j.cageo.2016.05.007

Langereis, C.G., Krijgsman, W., Muttoni, G., Menning, M. (2010). Magnetostratigraphy – concepts, definitions, and applications, *Newsletters on Stratigraphy*, *43*, 207-233.

López-Carmona, A., Abati, J., Pitra, P., & Lee, J. K. W. (2014). Retrogressed lawsonite blueschists from the NW Iberian Massif: P–T–t constraints from thermodynamic modelling and 40Ar/39Ar geochronology. *Contributions to Mineralogy and Petrology*, *167*(3), 987. https://doi.org/10.1007/s00410-014-0987-5

Mattei, M., Sagnotti, L., Faccenna, C., Funiciello, R. (1997). Magnetic fabric of weakly deformed clay-rich sediments in the Italian peninsula: Renlationship with compressional and extensional tectonics. *Tectonophysics*, 271, 107- 122. https://doi.org/10.1016/S0040-1951(96)00244-2

Martínez Catalán, J. R. (2012). The Central Iberian arc, an orocline centered in the Iberian Massif and some implications for the Variscan belt. *International Journal of Earth Sciences*, *101*(5), 1–16. https://doi.org/10.1007/s00531-011-0715-6

Martínez Catalán, J. R., Aerden, D. G. A. M., & Carreras, J. (2015). The “Castilian bend” of Rudolf Staub (1926): historical perspective of a forgotten orocline in Central Iberia. *Swiss Journal of Geosciences*, *108*(2–3), 289–303. https://doi.org/10.1007/s00015-015-0202-3

McFadden, P. L., & McElhinny, M. W. (1990). Classification of the reversals test in palaeomagnetism. Geophysical Journal International, 103(3), 725–729. https://doi.org/10.1111/j.1365-246X.1990.tb05683.x

McFadden, P. L., McElhinny, M. W., . (1988). The combined analysis of remagnetization circles and direct observations in palaeomagnetism. *Earth and Planetary Science Letters*, *87*(1–2), 161–172. https://doi.org/10.1016/0012-821X(88)90072-6

Merino-Tome, O., Bahamonde, J. R., Samankassou, E., & Villa, E. (2009). The influence of terrestrial run off on marine biotic communities: An example from a thrust-top carbonate ramp (Upper Pennsylvanian foreland basin, Picos de Europa, NW Spain). *Palaeogeography Palaeoclimatology Palaeoecology*, *278*(1–4), 1–23. Retrieved from http://www.elsevier.com

Nance, R. D., Gutiérrez-Alonso, G., Keppie, J. D., Linnemann, U., Murphy, J. B., Quesada, C., … Woodcock, N. H. (2010). Evolution of the Rheic Ocean. *Gondwana Research*, *17*(2–3), 194–222. https://doi.org/10.1016/j.gr.2009.08.001

Niocaill, C. Mac, & Mac Niocaill, C. (2000). A new Silurian palaeolatitude for eastern Avalonia and evidence for crustal rotations in the Avalonian margin of southwestern Ireland. *Geophysical Journal International*, *141*(3), 661–671. https://doi.org/10.1046/j.1365-246x.2000.00101.x

Ogg, J. G., Ogg, G., & Gradstein, F. M. (2016). A Concise Geologic Time Scale: 2016. Elsevier.

Pares, J. M. (2015). Sixty years of anisotropy of magnetic susceptibility in deformed sedimentary rocks. *Frontiers in Earth Science*, *3*(February), 1–13. https://doi.org/10.3389/feart.2015.00004

Pastor-Galán, D., Dekkers, M. J., Gutiérrez-Alonso, G., Brouwer, D., Groenewegen, T., Krijgsman, W., … Álvarez-Lobato, F. (2016). Paleomagnetism of the Central Iberian curve’s putative hinge: Too many oroclines in the Iberian Variscides. *Gondwana Research*, *39*, 96–113. https://doi.org/10.1016/j.gr.2016.06.016

Pastor-Galán, D., Groenewegen, T., Brouwer, D., Krijgsman, W., & Dekkers, M. J. (2015). One or two oroclines in the Variscan orogen of Iberia? Implications for Pangea amalgamation. *Geology*, *43*(6), 527–530. https://doi.org/10.1130/G36701.1

Pastor-Galán, D., Gutiérrez-Alonso, G., Mulchrone, K. F., & Huerta, P. (2012). Conical folding in the core of an orocline. A geometric analysis from the Cantabrian Arc (Variscan Belt of NW Iberia). *Journal of Structural Geology*, *39*. https://doi.org/10.1016/j.jsg.2012.02.010

Pastor-Galán, D., Ursem, B., Meere, P. A., & Langereis, C. (2015). Extending the Cantabrian Orocline to two continents (from Gondwana to Laurussia). Paleomagnetism from South Ireland. *Earth and Planetary Science Letters*, *432*. https://doi.org/10.1016/j.epsl.2015.10.019

Pastor-Galán, D., Mulchrone, K. F., Koymans, M. R., van Hinsbergen, D. J. J., & Langereis, C. G. (2017). Bootstrapped total least squares orocline test: A robust method to quantify vertical-axis rotation patterns in orogens, with examples from the Cantabrian and Aegean oroclines. *Lithosphere*, *9*(3). https://doi.org/10.1130/L547.1

Pastor-Galán, D., Gutiérrez-Alonso, G., Meere, P. A., & Mulchrone, K. F. (2009). Factors affecting finite strain estimation in low-grade, low-strain clastic rocks. *Journal of Structural Geology*, *31*(12), 1586–1596. https://doi.org/10.1016/j.jsg.2009.08.005

Pastor-Galán, D., Gutiérrez-Alonso, G., Fernández-Suárez, J., Murphy, J. B., & Nieto, F. (2013). Tectonic evolution of NW Iberia during the Paleozoic inferred from the geochemical record of detrital rocks in the Cantabrian Zone. *Lithos*, *182–183*. https://doi.org/10.1016/j.lithos.2013.09.007

Pastor-Galán, D., Gutiérrez-Alonso, G., & Weil, A. B. (2011). Orocline timing through joint analysis: Insights from the Ibero-Armorican Arc. *Tectonophysics*, *507*(1–4), 31–46. https://doi.org/10.1016/j.tecto.2011.05.005

Pastor-Galan, D., Gutierrez-Alonso, G., Zulauf, G., Zanella, F., Pastor-Galán, D., Gutiérrez-Alonso, G., … Zanella, F. (2012). Analogue modeling of lithospheric-scale orocline buckling: Constraints on the evolution of the Iberian-Armorican Arc. *Geological Society of America Bulletin*, *124*(7–8), 1293–1309. https://doi.org/10.1130/B30640.1

Pastor-Galán, D., Gutiérrez-Alonso, G., Dekkers, M.J. and Langereis, C.G., in press c, Paleomagnetism in Extremadura (Central Iberian zone, Spain) Paleozoic rocks: extensive remagnetizations and further constraints on the extent of the Cantabrian orocline. Journal of Iberian Geology, pp.1-18. https://doi.org/10.1007/s41513-017-0039-x

Pereira, M. F., Castro, A., Chichorro, M., Fernández, C., Díaz-Alvarado, J., Martí, J., & Rodríguez, C. (2014). Chronological link between deep-seated processes in magma chambers and eruptions: Permo-Carboniferous magmatism in the core of Pangaea (Southern Pyrenees). *Gondwana Research*, *25*(1), 290–308. https://doi.org/10.1016/j.gr.2013.03.009

Perez-Estaun, A., Bastida, F., Alonso, J. L., Marquinez, J., Aller, J., Alvarezmarron, J., … Pulgar, J. A. (1991). THE CANTABRIAN ZONE - AN INTERPRETATION FOR AN ARCUATE FORELAND THRUST BELT. *Tectonophysics*, *191*(3–4), 435.

Perini, G., Cebria, J. M., Lopez-Ruiz, J., & Doblas, M. (2004). Carboniferous-Permian mafic magmatism in the Variscan belt of Spain and France: implications for mantle sources. *Geological Society, London, Special Publications*, *223*(1), 415-438.

Pueyo, E. L.; Oliva-Urcia, B.; Sussman, A.J.; Cifelli, F. (2016). Palaeomagnetism in Fold and Thrust Belts: Use with caution. Geological Society of London Special Publication on Palaeomagnetism in Fold and Thrust Belts: New Perspectives. Edited by Pueyo, E.L.; Cifelli, F.; Sussman, A.; Oliva-Urcia, B., 425 (1), 259-276. doi:/10.1144/SP425.14

Ramón, M. J., Pueyo, E. L., Oliva-Urcia, B., & Larrasoaña, J. C. (2017). Virtual directions in paleomagnetism: A global and rapid approach to evaluate the NRM components. *Frontiers in Earth Science*, *5*, 8.

Roca, E., Guimerà, J., 1992. The Neogene structure of the eastern Iberian margin: structural constraints on the crustal evolution of the Valencia trough (western Mediterranean). Tectonophysics, 203, 203-218.

Sainz, A. M. C., & Faccenna, C. (2001). Tertiary compressional deformation of the Iberian plate. *Terra Nova*, *13*(4), 281–288. https://doi.org/10.1046/j.1365-3121.2001.00355.x

Salas, R., Casas, A., 1993. Mesozoic extensional tectonics, stratigraphy and crustal evolution during the Alpine cycle of the eastern Iberian basin. Tectonophysics, 228, 33-55.

Salas, R., Guimerà, J., Mas, R., Martín-Closas, C., Meléndez, A., Alonso, A., 2001. Evolution of the Mesozoic central Iberian Rift System and its Cainozoic inversion (Iberian chain). Mémoires du Museum national d'Histoire naturelle, 186, 145-186.

Seton, M., Müller, R. D. D., Zahirovic, S., Gaina, C., Torsvik, T., Shephard, G., … Chandler, M. (2012). Global continental and ocean basin reconstructions since 200Ma. *Earth-Science Reviews*, *113*(3–4), 212–270. https://doi.org/10.1016/j.earscirev.2012.03.002

Shaw, J., Johnston, S. T., Gutiérrez-Alonso, G., Weil, A. B., Gutiérrez-Alonso, G., & Weil, A. B. (2012). Oroclines of the Variscan orogen of Iberia: Paleocurrent analysis and paleogeographic implications. *Earth and Planetary Science Letters*, *329–330*, 60–70. https://doi.org/10.1016/j.epsl.2012.02.014

Simón Gómez, J.L., 1982. Compresión y distensión alpinas en la Cadena Ibérica oriental. Tesis Doctoral. Universidad de Zaragoza. 501 pp.

Staub, R. (1926). *Gedanken zur Tektonik Spaniens. Vierteljahrss- chrift der Naturforschenden Gesellschaft*, (Vol. 71). Zürich.

Tarling, D. and Hrouda, F. eds., 1993. Magnetic anisotropy of rocks. Springer Science & Business Media.

Tauxe, L. (2010). Essentials of paleomagnetism. Retrieved from https://scholar.google.com/scholar?cluster=6824168530500552667&hl=en&oi=scholarr#0

Tauxe, L., & Watson, G. S. (1994). The fold test: an eigen analysis approach, *122*, 331–341.

Torsvik, T. H., Voo, R. Van Der, Preeden, U., Mac, C., Steinberger, B., Doubrovine, P. V, … Cocks, L. R. M. (2012). Phanerozoic polar wander, palaeogeography and dynamics. *Earth-Science Reviews*, *114*(3–4), 325–368. https://doi.org/10.1016/j.earscirev.2012.06.007

Van der Voo, R. (1990). The reliability of paleomagnetic data. Tectonophysics, 184(1), 1-9.

Veevers, J. J. (2004). Gondwanaland from 650-500 Ma assembly through 320 Ma merger in Pangea to 185-100 Ma breakup: supercontinental tectonics via stratigraphy and radiometric dating. *Earth-Science Reviews*, *68*(1–2), 1–132.

Velzen, A. J., & Zijderveld, J. D. A. (1995). Effects of weathering on single-domain magnetite in Early Pliocene marine marls. *Geophysical Journal International*, *121*(1), 267–278. https://doi.org/10.1111/j.1365-246X.1995.tb03526.x

Villas, E. (1995). Caradoc through Early Ashgill Brachiopods from the Central-Iberian zone (Central Spain). *Geobios*, *28*(1), 49-84.

Vissers, R. L. M., van Hinsbergen, D. J. J., van der Meer, D. G., & Spakman, W. (2016). Cretaceous slab break-off in the Pyrenees: Iberian plate kinematics in paleomagnetic and mantle reference frames. *Gondwana Research*, *34*, 49–59. https://doi.org/10.1016/J.GR.2016.03.006

Weil, A. B., Gutiérrez-Alonso, G., & Conan, J. (2010). New time constraints on lithospheric-scale oroclinal bending of the Ibero-Armorican Arc: a palaeomagnetic study of earliest Permian rocks from Iberia. *Journal of the Geological Society*, *167*(1), 127–143. https://doi.org/10.1144/0016-76492009-002

Weil, A. B., Gutiérrez-Alonso, G., Johnston, S. T., & Pastor-Galán, D. (2013). Kinematic constraints on buckling a lithospheric-scale orocline along the northern margin of Gondwana: A geologic synthesis. *Tectonophysics*, *582*. https://doi.org/10.1016/j.tecto.2012.10.006

Weil, A. B., & Yonkee, A. (2009). Anisotropy of magnetic susceptibility in weakly deformed red beds from the Wyoming salient, Sevier thrust belt: Relations to layer-parallel shortening and orogenic curvature. *Lithosphere*, *1*(4), 235–256. https://doi.org/10.1130/L42.1

Zijderveld, J. D. A. (1967). A.C. demagnetization of rocks: analysis of results. In D. Collisnson, K. Creer, & S. Runcorn (Eds.), *Methods of Paleomagnetism* (pp. 254–286). Amsterdam: Elsevier.

Captions

Fig. 1 A) Location of the main Variscan orogeny outcrops in western Europe with Iberia restored to a pre-Albian rotation (Gong et al., 2008). B) Simplified geological map of the Iberian Range after García-Lasanta et al. (2017), highlighting the Paleozoic outcrops and the studied area.

Fig. 2 Structure and lithology of the Santa Cruz syncline. A) Pi diagram showing all the bedding measurements taken and the fold axis attitude. B) AMS fabrics showing a sedimentary magnetic fabric (k_{min} is perpendicular to bedding) with a slight tectonic fabric (k_{max} is subparallel to the fold axis). C) Geological map of the studied area and location of the samples collected.

Fig. 3 Representative Zijderveld diagrams and great circle approach in the studied samples.

Fig. 4 Component P directions and VGPs in geographic coordinates for sediments (left) and dykes and sill (right).

Fig. 5 A) Component #1 directions and VGPs in geographic coordinates. B) Negative fold test indicating the post-folding origin of the component.

Fig. 6 A) Component #2 directions and VGPs in structurally corrected coordinates. B) Component #2 directions in geographic coordinates (note the high dispersion) and positive fold test, which indicates the pre-folding character of this component. C) Positive reversal test between both normal and reverse directions found in Component #2, suggesting a pre-Kiaman magnetization of the studied rocks.

Fig. 7 Cartoon depicting the different vertical axis rotation events that occurred in the Iberian Range. A) Original quasi-linear Variscan belt. B) The formation of the Cantabrian Orocline at the

Carboniferous-Permian limit involved a ~70˚ CCW rotation in the area which fully corresponds with the expected rotation, considering the strike of the Variscan structures in the Iberian Range as shown by the perfect fit of Component #2 in the orocline test for the Cantabrian Zone (below). C) Cenozoic rotation of ~22˚ CW likely produced by differential shortening during the Alpine Orogeny (Izquierdo-Llavall et al., 2018). Note that once this 22˚ CW rotation is corrected, both Components #2, #1 and P fit perfectly with the APWP for the southern limb of the orocline (Pastor-Galán et al., 2016). Below, the Global Magnetic Polarity Time Scale for the Pennsylvanian and Cisselian (following Ogg et al., 2016)

Fig. 8 GAPWaP (Torsvik et al., 2012) adapted to the Euler pole rotations chosen to reconstruct Iberia and a paleomagnetic compilation of Iberian poles from Dinarés et al., 2005, Vissers et al., 2016 and Pastor-Galán et al., 2016, in press c.

Fig. 9 Gplates reconstruction of the Late Carboniferous-Early Permian rotation linked with the Cantabrian Orocline formation in Iberia with Europe fixed (modified from Domeier and Torsvik, 2014). Note that we considered Iberia and the rest of Pangea rigid to account for the missing deformation, and therefore this map does not show a paleogeography. The calculated shortening (either below Europe or Iberia) exceeds 1000 km.

Table 1 Paleomagnetic results and statistical information for each component.

Table 2 Euler poles to adapt GAPWaP for Africa (Torsvik et al., 2012) to the Iberian plate as shown in Figure 8.

Supplementary files

SF1 KLM file with the location of each site

SF2 Extra AMS plots

SF3 Raw and interpreted paleomagnetic data. All this data can be opened in Paleomagnetism.org

SF4 Thermomagnetic curves for different specimens. Magnetization in most specimens is carried by (Ti-)magnetite. MD14 shows a clear hematite carrier and some samples present some pyrite.

SF5 Positive reversal test and CMTD test comparing Component #2 with the C component of Pastor-Galán et al., 2016.

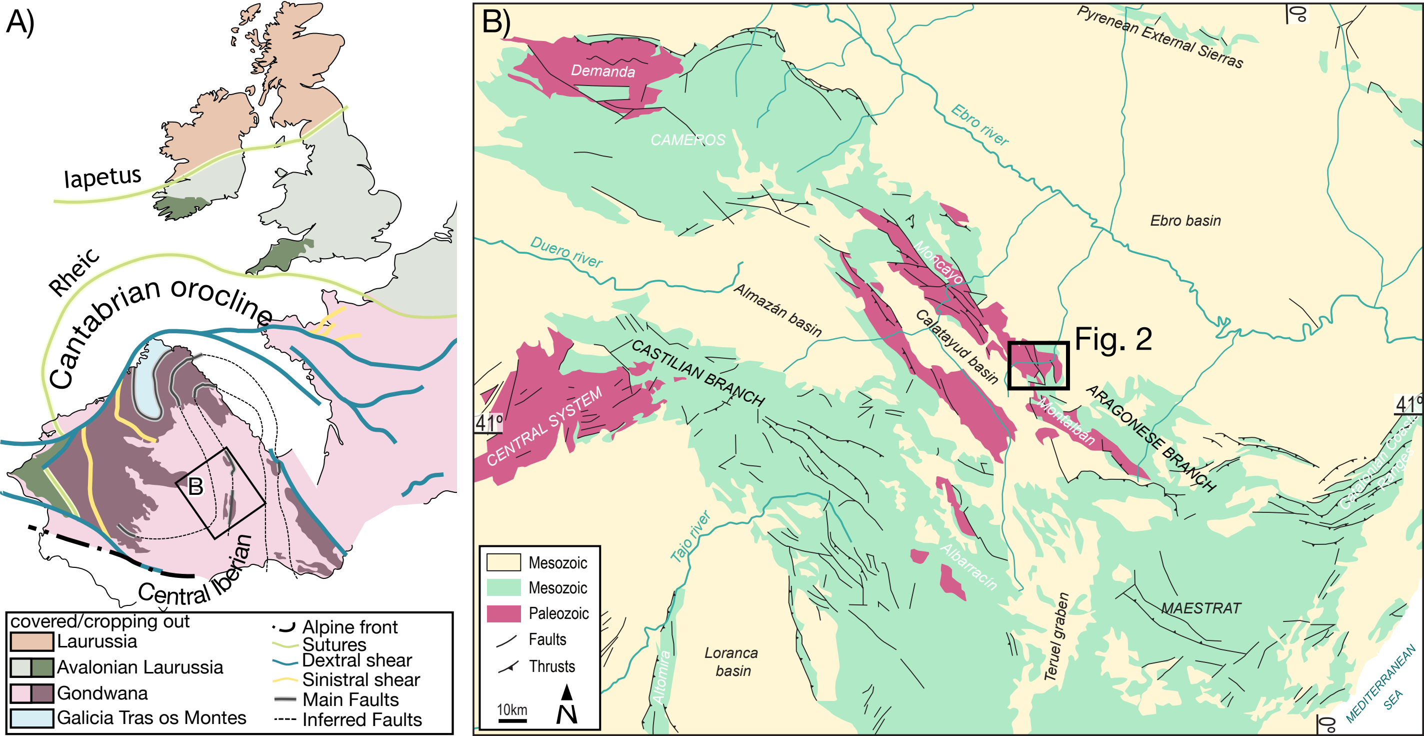
A)
Iapetus
Rheic
Cantabrian orocline
B
Central Iberian
covered/cropping out
Laurussia
Avalonian Laurussia
Gondwana
Galicia Tras os Montes
Alpine front
Sutures
Dextral shear
Sinistral shear
Main Faults
Inferred Faults
B)
Demanda
CAMEROS
Pyrenean External Sierras
Ebro river
Ebro basin
Duero river
Moncayo
Almazán basin
Calatayud basin
Fig. 2
CASTILIAN BRANCH
ARAGONESE BRANCH
CENTRAL SYSTEM
Montalbán
41°
41°
0°
0°
Catalonian Coastal Ranges
Tajo river
Albarracín
Teruel graben
MAESTRAT
Loranca basin
Altomira
MEDITERRANEAN SEA
Mesozoic
Mesozoic
Paleozoic
Faults
Thrusts
10km
N

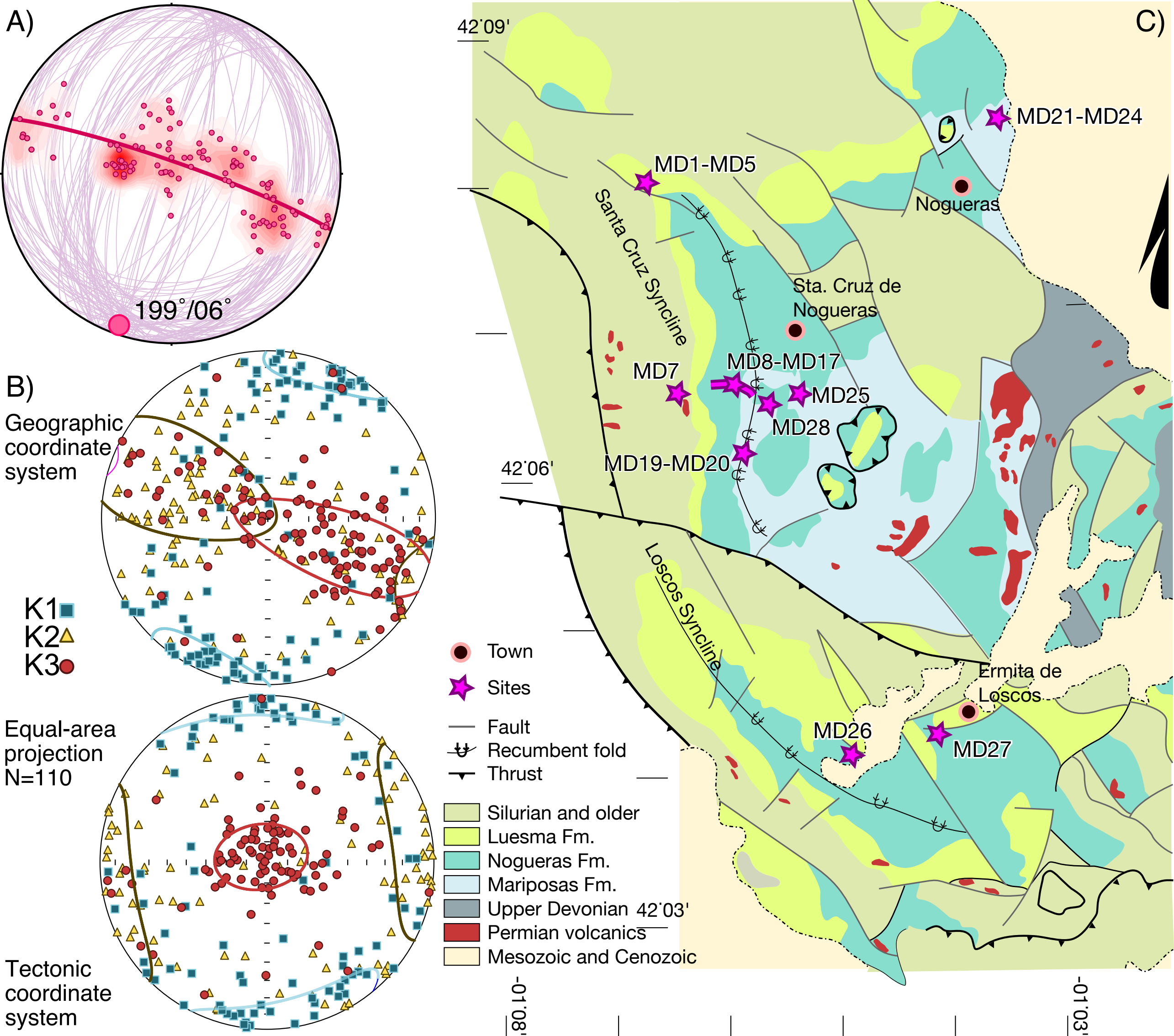
A)
199˚/06˚
B)
Geographic coordinate system
K1
K2
K3
Equal-area projection N=110
Tectonic coordinate system
C)
42˚09'
42˚06'
42˚03'
-01˚08'
-01˚03'
MD21-MD24
MD1-MD5
Nogueras
Santa Cruz Syncline
Sta. Cruz de Nogueras
MD7
MD8-MD17
MD25
MD28
MD19-MD20
Loscos Syncline
Ermita de Loscos
MD26
MD27
Town
Sites
Fault
Recumbent fold
Thrust
Silurian and older
Luesma Fm.
Nogueras Fm.
Mariposas Fm.
Upper Devonian
Permian volcanics
Mesozoic and Cenozoic

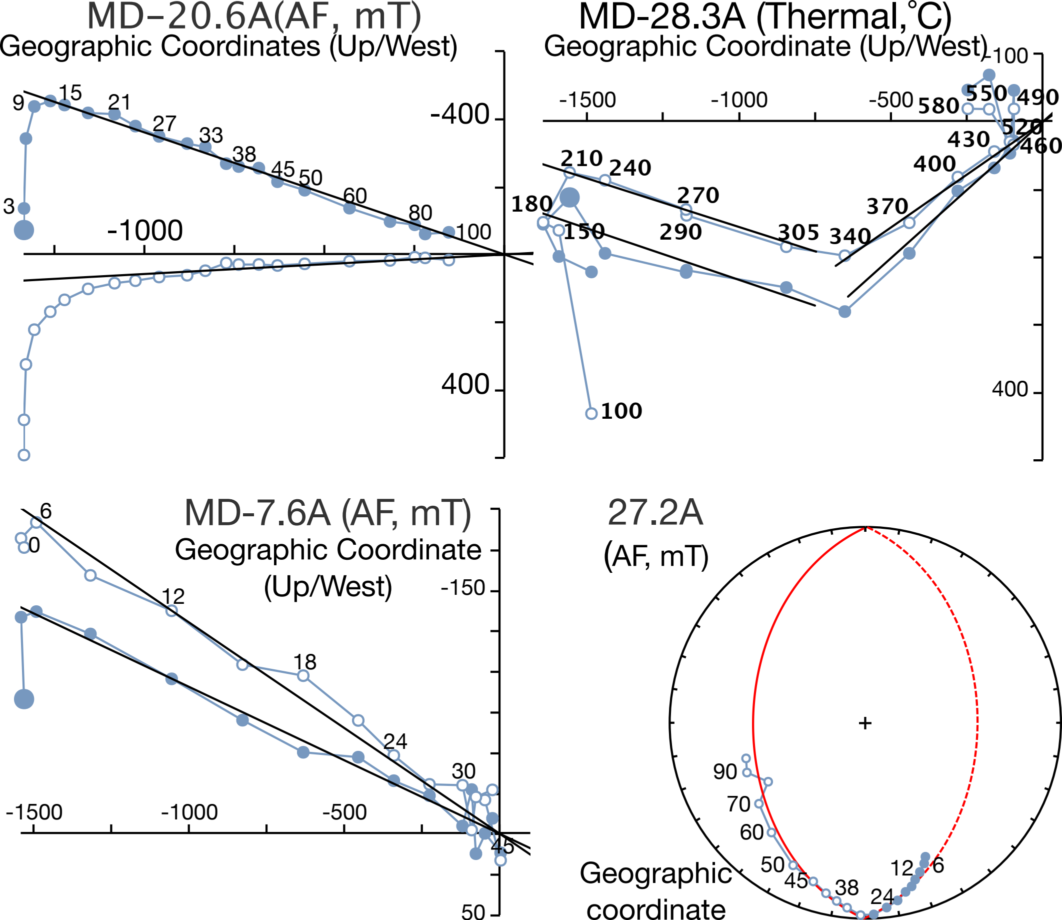
MD–20.6A(AF, mT)
Geographic Coordinates (Up/West)
-400
-1000
400
3
9
15
21
27
33
38
45
50
60
80
100
MD-28.3A (Thermal,°C)
Geographic Coordinate (Up/West)
-1500
-1000
-500
-100
400
100
150
180
210
240
270
290
305
340
370
400
430
460
490
520
550
580
MD-7.6A (AF, mT)
Geographic Coordinate
(Up/West)
-150
50
-1500
-1000
-500
0
6
12
18
24
30
45
27.2A
(AF, mT)
Geographic
coordinate
90
70
60
50
45
38
24
12
6

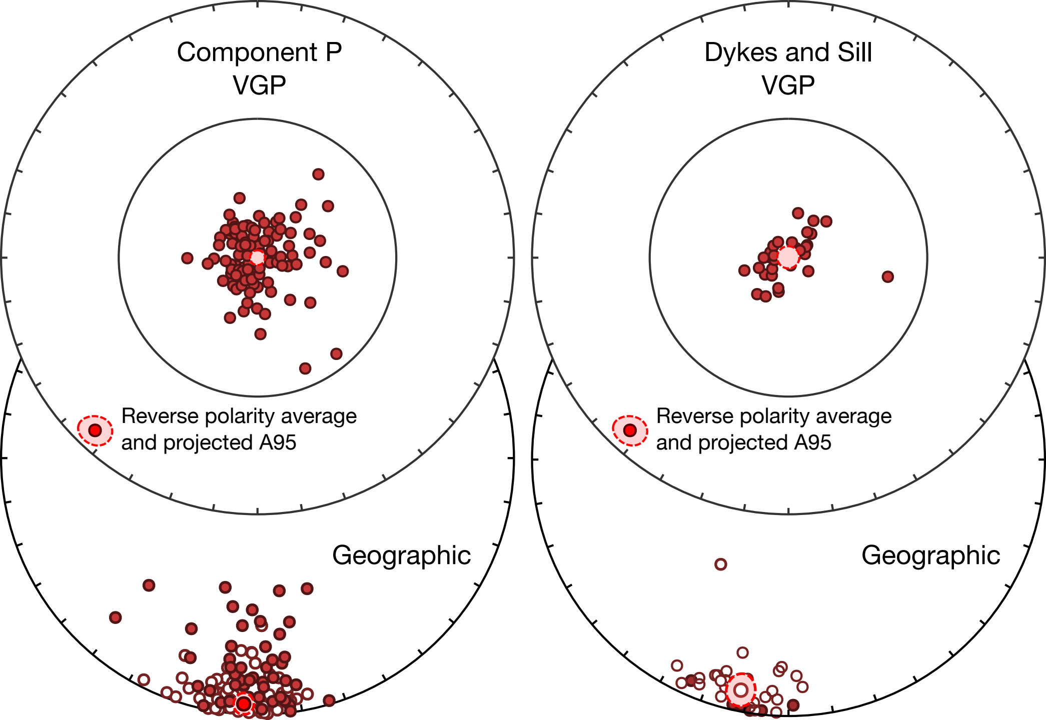

Component P
VGP
Reverse polarity average
and projected A95
Geographic
Dykes and Sill
VGP
Reverse polarity average
and projected A95
Geographic

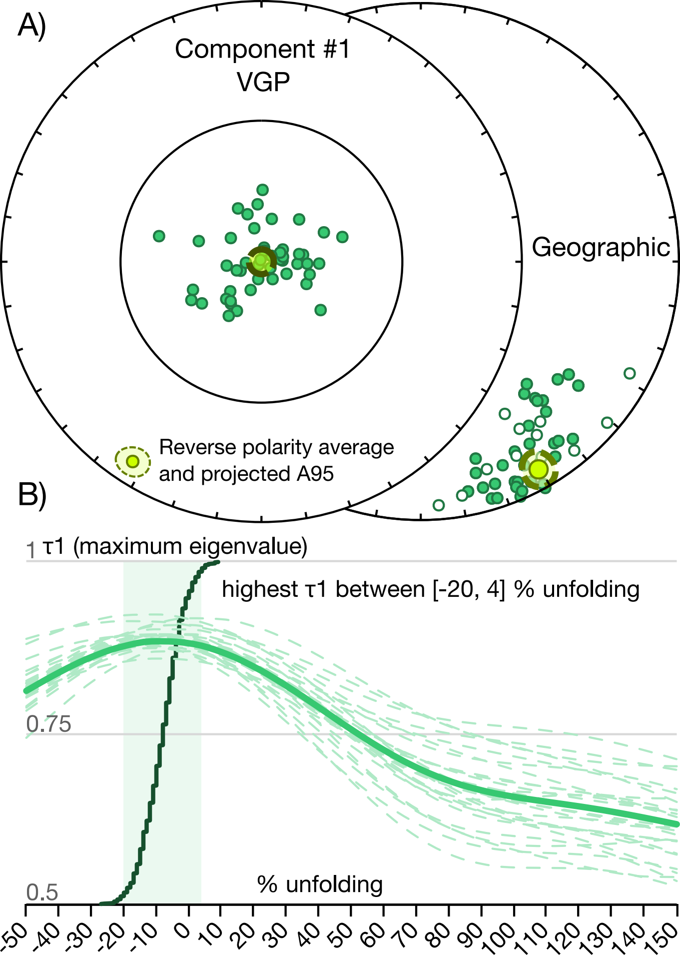
A)
Component #1
VGP
Geographic
Reverse polarity average
and projected A95
B)
1 τ1 (maximum eigenvalue)
highest τ1 between [-20, 4] % unfolding
0.75
0.5
% unfolding
-50
-40
-30
-20
-10
0
10
20
30
40
50
60
70
80
90
100
110
120
130
140
150

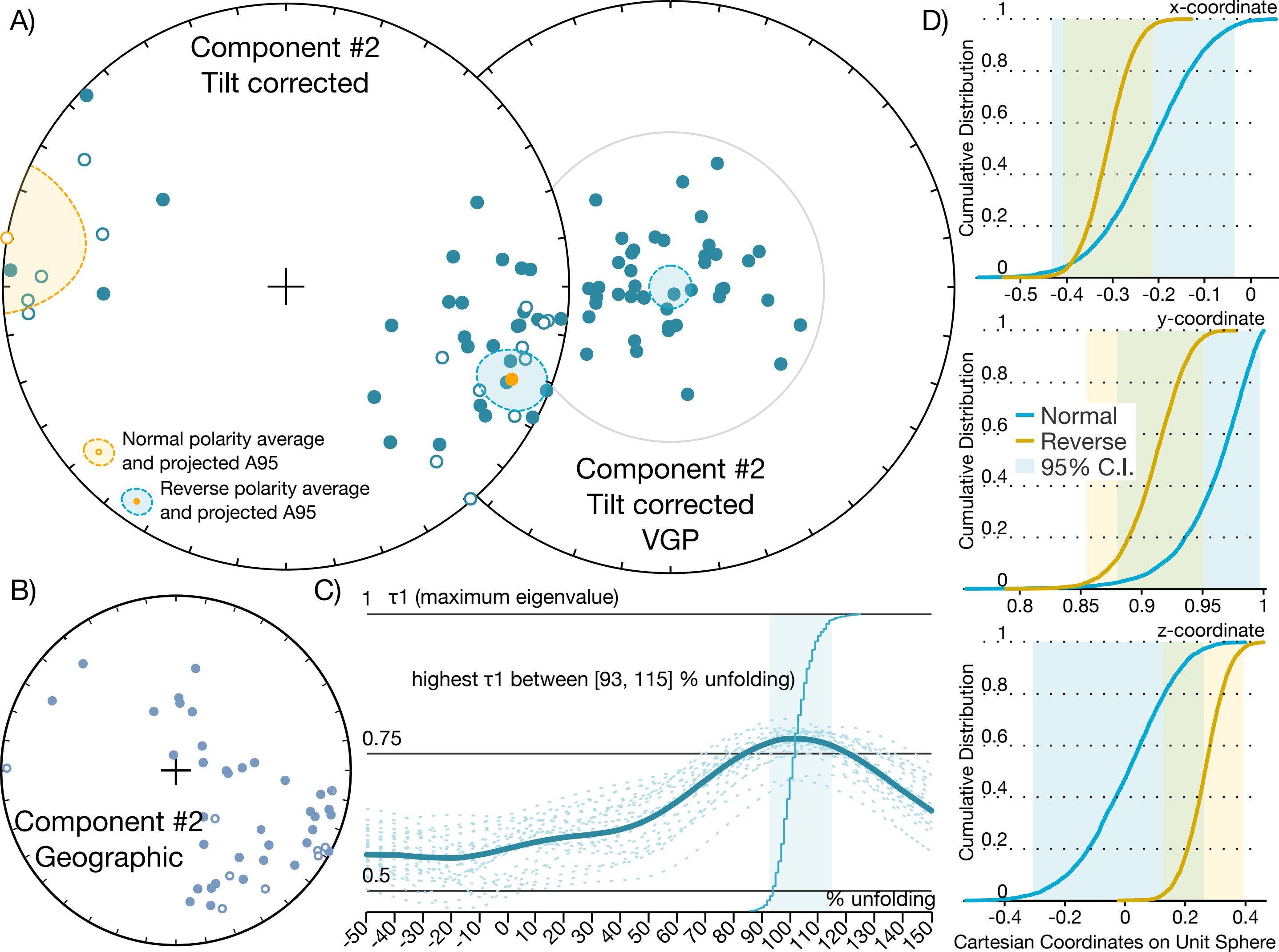

A)
Component #2
Tilt corrected
Normal polarity average
and projected A95
Reverse polarity average
and projected A95
Component #2
Tilt corrected
VGP
B)
Component #2
Geographic
C)
1 τ1 (maximum eigenvalue)
highest τ1 between [93, 115] % unfolding)
0.75
0.5
% unfolding
-50 -40 -30 -20 -10 0 10 20 30 40 50 60 70 80 90 100 110 120 130 140 150
D)
x-coordinate
y-coordinate
z-coordinate
Cumulative Distribution
Normal
Reverse
95% C.I.
Cartesian Coordinates on Unit Sphere

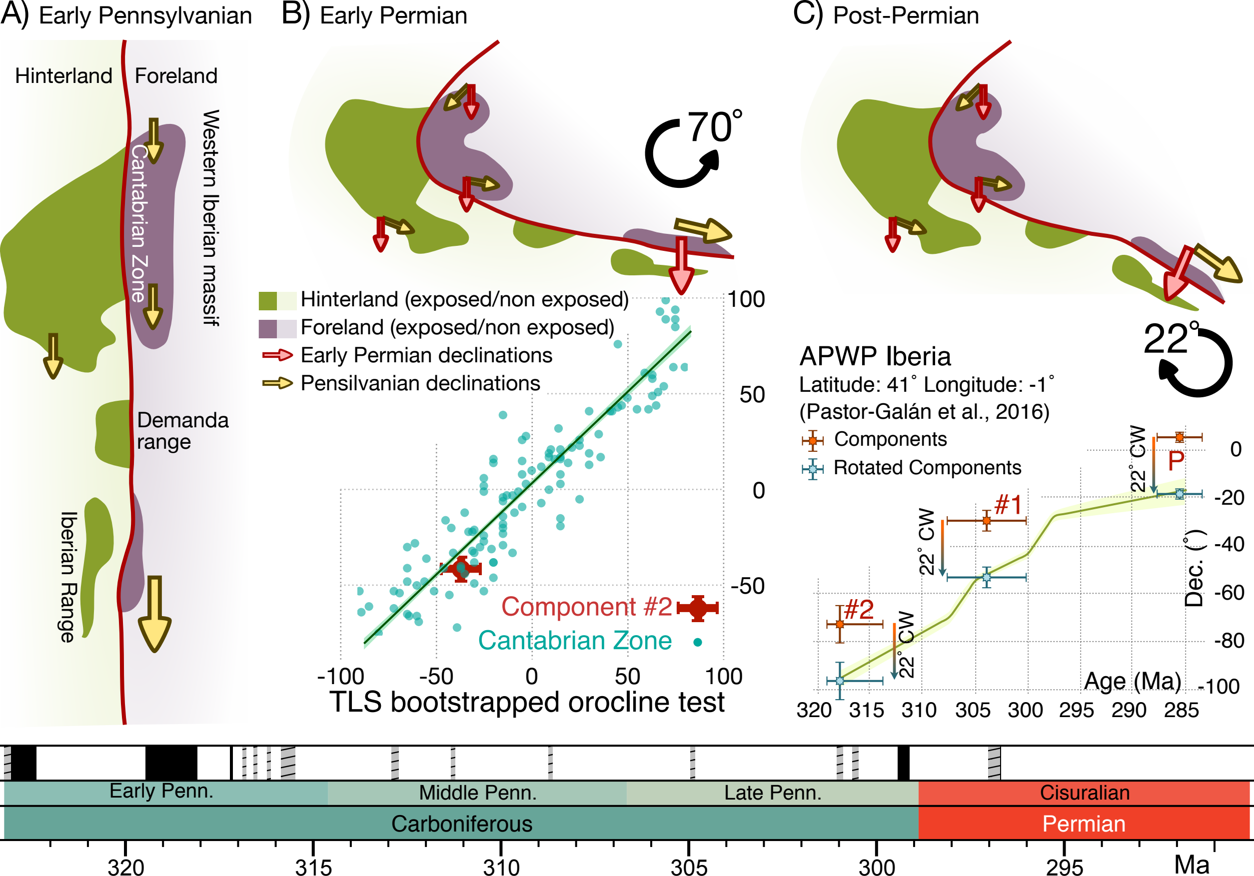

A) Early Pennsylvanian
B) Early Permian
C) Post-Permian
Hinterland
Foreland
Western Iberian massif
Cantabrian Zone
Demanda range
Iberian Range
70°
22°
Hinterland (exposed/non exposed)
Foreland (exposed/non exposed)
Early Permian declinations
Pensilvanian declinations
Component #2
Cantabrian Zone
TLS bootstrapped orocline test
APWP Iberia
Latitude: 41° Longitude: -1°
(Pastor-Galán et al., 2016)
Components
Rotated Components
#1
#2
P
22° CW
Dec. (°)
Age (Ma)
Early Penn.
Middle Penn.
Late Penn.
Cisuralian
Carboniferous
Permian
Ma

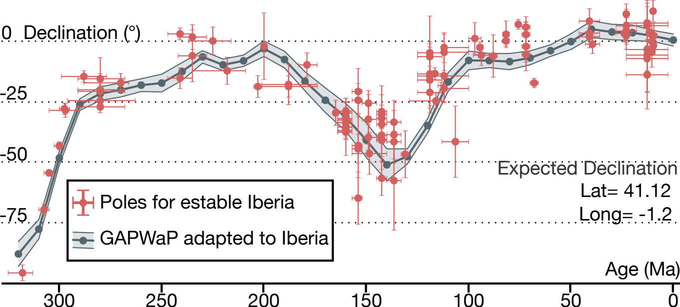
0 Declination (°)
-25
-50
-75
Expected Declination
Lat= 41.12
Long= -1.2
Poles for estable Iberia
GAPWaP adapted to Iberia
Age (Ma)
300
250
200
150
100
50
0


315 Ma
America
-10°
315 Ma
Europe
Minimum
shortened area
Africa
315 Ma
305 Ma
295 Ma
285 Ma
285 Ma
0°
Minimum
extended
area
285 Ma